Catal Lett (2008) 122:259–266
DOI 10.1007/s10562-007-9373-5

Control of the Basicity in Ni–MgO Systems: Influence in the Hydrogenation of Styrene Oxide

Olga Bergadà · Pilar Salagre · Yolanda Cesteros · Francisco Medina · Jesús E. Sueiras

Received: 1 August 2007 / Accepted: 17 November 2007 / Published online: 11 December 2007

Abstract The addition of basic solutions to the reaction medium in the catalytic hydrogenation of styrene oxide improves the selectivity to 2-phenylethanol (used in perfumery) but also can favour condensation reactions. To study the influence of different basic sites on the reaction products, we prepared several catalysts by mixing a commercial magnesia (MgO), and other previously rehydrated (MgOr), with different amounts of NiO followed by reduction (NiMgO, 4NiMgO, NiMgOr, 4NiMgOr), and by mixing directly MgO with Ni (NiMgOa, 4NiMgOa). Ni–MgO catalysts showed the best conversion and selectivity to 2-phenylethanol values, arriving to 100% when increasing the MgO content. Interestingly, CO_2-TPD study of catalyst NiMgO indicates that metallic nickel covers the weakest basic sites of magnesia. On the other hand, CO_2-TPD profiles of Ni–MgOr and Ni–MgOa catalysts, which present low catalytic activity, showed an important amount of available basic sites that favour the formation of higher amounts of condensation products, which are responsible for the catalyst deactivation.

Keywords Basicity · Styrene oxide hydrogenation · 2-Phenylethanol · CO_2-TPD

O. Bergadà · P. Salagre · Y. Cesteros
Facultat de Química, Universitat Rovira i Virgili, C/Marcel·lí Domingo s/n, 43007 Tarragona, Spain

P. Salagre (✉)
Departament de Química Física i Inorgànica, Universitat Rovira i Virgili, C/Marcel·lí Domingo s/n, 43007 Tarragona, Spain
e-mail: pilar.salagre@urv.net

F. Medina · J. E. Sueiras
Escola Tècnica Superior d'Enginyeria Química, Universitat Rovira i Virgili, Av. Països Catalans, 26, 43007 Tarragona, Spain

1 Introduction

2-Phenylethanol is the main component of the rose oils obtained from rose blossoms. This alcohol is widely used as component in all chemical perfumes and as additive in foods due to its pleasant smell [1].

Nowadays, 2-phenylethanol is industrially produced by different processes, which generate economical and environmental important problems. Thus, one of the methods used consists of reacting chlorobenzene with Grignard-type reactants, followed by several reaction steps, which finally give to the formation of 2-phenylethanol, with a low degree of purity, and high amounts of pollutant wastes [2, 3]. Other method to obtain this alcohol is the Friedel–Crafts alkylation of benzene with ethylene oxide, using molar amounts of aluminium chloride as catalyst [4, 5]. The highly corrosive species formed together with the great difficulty to recover the catalyst constitute the main disadvantages of this method. This impure 2-phenylethanol becomes unusable for the industry of perfume.

An alternative to all these industrial processes should be more selective and at the same time more respectful with the environment. The catalytic hydrogenation of styrene oxide for the selective obtention of 2-phenylethanol is an environmental friendly process that has been studied from 50 years [6, 7] in order to solve the pollution and economical problems generated with the usual industrial methods.

Bulk nickel, palladium and platinum catalysts have shown to be good catalysts for this reaction [8–10]. Their activity and selectivity were considerably improved with the addition of basic solutions to the reaction medium (88% of selectivity to 2-phenylethanol for a 95% of conversion for a Raney–Ni catalyst) [8]. From these results, Mitsui

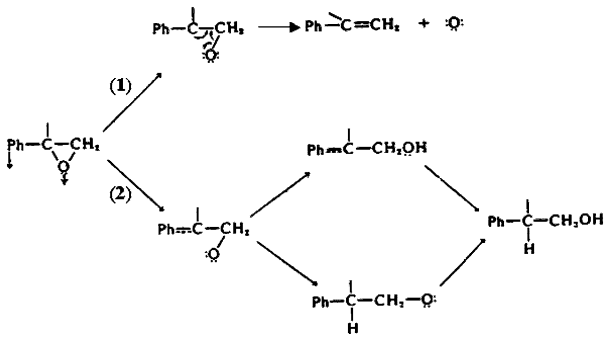

Scheme 1 Mechanism of the styrene oxide hydrogenation

et al. proposed that this basic solution decreases the interaction between the oxygen of styrene oxide and the catalytic surface minimizing the ethylbenzene formation (way 1), and favouring the obtention of 2-phenylethanol (way 2) (see Scheme 1). However, the basic medium could also favour condensation reactions [10]. In the literature, we found that magnesium oxide has been used as catalytic support and as basic catalyst in a great variety of reactions [11–14]. The key factor in obtaining oxides with different properties is the use of different preparative methods [15, 16]. In a previous work, we tested bulk Ni and Ni–MgO catalysts for the hydrogenation of styrene oxide, and total conversion (100%) and high selectivity to 2-phenylethanol (100%) were obtained with the Ni–MgO systems [13].

The aim of this work is to study the influence of different basic sites, in Ni–MgO systems, on the reaction products distribution obtained in the hydrogenation of styrene oxide. To obtain this information, we have prepared several Ni–MgO catalysts modifying: (a) the basic solid used (commercial MgO and rehydrated MgO), (b) the metallic nickel amount, and (c) the distribution of basic and nickel sites by using two preparative methods. The catalytic results will be correlated with CO_2-TPD studies.

2 Experimental

2.1 Catalysts Preparation

Commercial $Ni(NO_3)_2{\cdot}6H_2O$ (Panreac, 99%) was thermally decomposed flowing Ar through the sample (120 cm^3/min) at 180 °C until $Ni(NO_3)_2$ was obtained as a single phase (6 h). This was later calcined at 320 °C for 6 h to obtain the NiO sample.

Rehydrated magnesia (MgOr) was prepared by refluxing commercial MgO (Aldrich 99%, 130 m^2/g) in distilled water for 1 h. Then, the solid was filtered and dried at 120 °C overnight.

NiO/MgO and NiO/MgOr systems were obtained with different weight ratios (1:1 and 4:1) from physical mixtures of the NiO sample (previously prepared) with commercial magnesia (MgO), or rehydrated magnesia (MgOr), respectively, by stirring the mixture in cyclohexane for 1 h at room temperature. The organic solvent was then evaporated. These catalytic precursors are named as NiOMgO, 4NiOMgO, NiOMgOr and 4NiOMgOr.

These NiO/MgO and NiO/MgOr systems were reduced with pure H_2 at 250 °C for 4 h to obtain the corresponding catalysts (NiMgO, 4NiMgO, NiMgOr, 4NiMgOr). Also, one catalyst without MgO was obtained by reduction of the NiO sample, previously prepared, with pure H_2 at 250 °C for 2 h (Ni sample). Lastly, two catalysts with Ni/MgO weight ratios of 1:1 and 4:1 (catalysts NiMgOa, 4NiMgOa) were prepared from physical mixtures of commercial MgO with metallic Ni (Ni sample) by stirring in degassed cyclohexane at room temperature for 1 h, and later evaporation of the solvent.

2.2 Air-free Sampling

The catalysts were always handled under air-free conditions after the reduction step. The catalysts were transferred in degassed cyclohexane and under a hydrogen atmosphere at room temperature. The cyclohexane surface-impregnated samples were further isolated from the air with sticky tape for X-ray diffraction (XRD) monitoring, where a glove box was used for mounting.

2.3 Infrared Spectroscopy

Infrared spectra were recorded on a Bruker-Equinox-55 FTIR spectrometer. The spectra were acquired by accumulating 32 scans at 4 cm^{-1} resolution in the range 400–4000 cm^{-1}. Samples were prepared by mixing the powdered solids with pressed KBr disks (blank) in a ratio of 15:85.

2.4 X-ray Diffraction

Powder X-ray diffraction patterns of the different samples were obtained with a Siemens D5000 diffractometer using nickel-filtered Cu Kα radiation. Samples were dusted on double-sided sticky tape and mounted on glass microscope slides. The patterns were recorded over a range of 2θ angles from 10 to 90° and crystalline phases were identified using the Joint Committee on Powder Diffraction Standards (JCPDS) files: 04-0850-Nickel, syn-Ni; 04-0835-Bunsenite, syn-NiO; 45-0946-Periclase, syn-MgO,

44-1482 $Mg(OH)_2$ Brucite. From the diffraction data, crystallite sizes were determined by using the Scherrer equation for all samples.

2.5 BET Areas

BET areas were calculated from the nitrogen adsorption isotherms at 77 K using a Micromeritics ASAP 2000 surface analyser and a value of 0.164 nm^2 for the cross-section of the nitrogen molecule.

2.6 Temperature-programmed Reduction

Temperature-programmed reductions (TPR) were carried out in a Perkin-Elmer TGA 7 microbalance equipped with a 0–1000 °C programmable temperature furnace. The accuracy was ±1 μg. Each sample (30 mg) was heated in a 5 vol% H_2/Ar flow (80 cm^3/min) from 50 to 627 °C at 15 °C/min.

2.7 Scanning Electron Microscopy

Scanning electron micrographs (SEM) were obtained with a JEOL JSM-35C scanning microscope operating at an accelerating voltage in the range 15–25 kV, work distance (wd) of 14 mm and magnification values in the range 40,000–50,000×.

2.8 Temperature-programmed Desorption-mass Spectrometry Experiments (CO_2-TPD)

The basic properties of the solids were characterized by TPD of CO_2 using a TPD/R/O 1100 (Thermo Finnigan) equipped with a programmable temperature furnace and a calibrated TCD detector. The gas outlet was coupled to a quadrupole mass spectrometer Pfeiffer GSD300. Experiments were performed with 3% CO_2/He flowing though the sample which was previously dried. The desorption of CO_2 was made by flowing He 20 cm^3/min from room temperature to 700 °C at 5 °C/min.

2.9 Hydrogen Chemisorption

The hydrogen chemisorption was measured with a Micromeritics ASAP 2010C instrument. Samples were previously reduced under the same conditions as for preparing the catalysts. After reduction, the hydrogen on the nickel surface was removed with 15 mL min^{-1} of N_2 for 30 min at 350 °C The sample was subsequently cooled to room temperature under the same N_2 stream and H_2 pulses (0.047 mL) were injected until the eluted area of consecutive pulses was constant. The nickel surface atoms were calculated assuming a stoichiometry of one hydrogen molecule adsorbed per two surface nickel atoms.

2.10 Catalytic Activity Determination

The catalytic hydrogenation of styrene oxide was made in the liquid phase, using for all tests 0.5 g of active phase, 20 mL of absolute ethanol (Panreac, 99.5%) and 4 mmol of styrene oxide (Aldrich, 97%) with a hydrogen flow of 120 cm^3/min and agitation of 700 rpm. The reaction was performed at room temperature. Sample was taken each 1, 3 and 6 h. The reaction products were analyzed by gas chromatography, using a chromatograph Shimadzu GC-2010 with 30 m of capillary column "DB-1" and a FID detector. They were quantified by adding an internal standard and by using a calibrated line. We also tested the catalytic lifetime of the best catalyst by reusing the catalyst five times at the same catalytic conditions.

3 Results and Discussion

3.1 Characterization of the Catalytic Precursors and Catalysts

The rehydrated sample (MgOr) was characterized by infrared spectroscopy in order to determine the presence of hydroxyl groups. Figure 1 shows the IR spectrum for this sample where an intense band appeared at 3,698 cm^{-1}, corresponding to hydroxyl groups, indicates the rehydration of magnesia. XRD pattern of MgOr (not shown here) confirms the complete transformation of periclase to brucite ($Mg(OH)_2$) after the rehydration process.

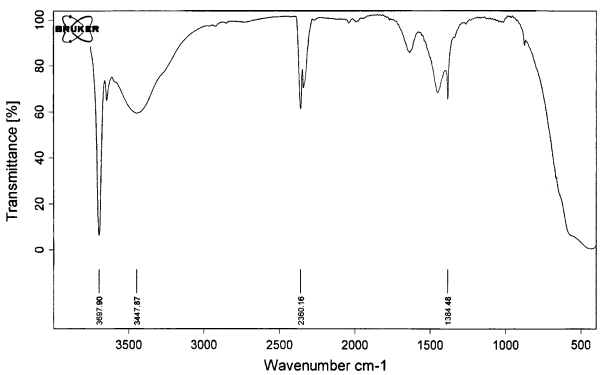

Fig. 1 Infrared spectrum of rehydrated magnesia

Table 1 Characterization of MgO, MgOr and the catalytic precursors

Samples	Crystalline phases (XRD)	BET area (m^2/g)	Average crystallite size (nm)[a]	T_R (°C)[b]
MgO	MgO	130	16.9	–
MgOr	$Mg(OH)_2$	73	19.4	–
NiO	NiO	43	23.3	346
NiOMgO	NiO, MgO	93	23.2[c]	371
4NiOMgO	NiO, MgO	67	23.5[c]	354
NiOMgOr	NiO, $Mg(OH)_2$	56	23.3[c]	363
4NiOMgOr	NiO, $Mg(OH)_2$	48	23.3[c]	348

[a] Using the Scherrer equation

[b] Initial reduction temperature obtained from TPR experiments

[c] Calculated for the NiO phase

Table 1 shows several characterization data for the catalytic precursors. Powder diffraction patterns of the NiO–MgO precursors exhibit NiO and MgO phases, whereas for the NiO–MgOr systems, NiO and $Mg(OH)_2$ phases were observed. The presence of two phases indicates that there is not solid solution in these catalytic precursors and, therefore, NiO–MgO and NiO–$Mg(OH)_2$ interactions are low [16]. Taking into account that the average crystallite size for the NiO sample is 23.3 nm and for the commercial MgO and sample MgOr are 16.9 and 19.4 nm, respectively, we observe that the NiO average crystallite size values practically did not change during the mixture process (Table 1).

The BET area values observed for the MgO and MgOr samples are 130 and 73 m^2/g, respectively (Table 1). All the catalytic precursors show BET area values proportional to the amount of added magnesia. Thus, the sample with higher magnesia content (NiOMgO) has the highest surface area (Table 1). The precursors with MgOr exhibit lower surface areas than the precursors with commercial MgO (Table 1). These results were expected due to the lower surface area obtained for the MgOr sample.

In order to compare the reducibility of the catalytic precursors, we take from TPR experiments the temperature at what the NiO starts to reduce (initial reduction temperature). In a previous work, the initial reduction temperature (T_R) for the NiO precursor was determined as 346 °C [13]. NiO–MgO and NiO–MgOr systems show higher initial reduction temperature than the NiO precursor being the samples with commercial magnesia those that have higher T_R value (Table 1). These results let us to think that there is a certain interaction between NiO and MgO, and between NiO and $Mg(OH)_2$, respectively. This interaction is slightly higher for the catalytic precursors with magnesia. Thus, the system with higher amount of commercial magnesia (NiMgO) presents the highest initial reduction temperature (Table 1).

SEM was used to monitor the morphology of the particles for the catalytic precursors. All the precursors prepared with commercial magnesia and with rehydrated magnesia show some particles with a certain octahedral morphology that should correspond to NiO (Fig. 2a, b). Additionally, the samples with MgOr exhibit particles with lamellar morphology corresponding to the brucite phase (Fig. 2b).

Once reduced, all NiO is converted to crystalline metallic nickel for all catalysts, as observed by XRD, together with the corresponding MgO or $Mg(OH)_2$ phase (Table 2). The metallic areas of the catalysts are also shown in Table 2. For the catalysts with MgOr (NiMgOr and 4NiMgOr) and for the catalyst 4NiMgO, we observe lower metallic areas than for the catalysts prepared by mixing Ni with MgO (NiMgOa, 4NiMgOa). This can be related to the water formed during the reduction process that should give to some agglomeration of the periclase or brucite particles due to the hygroscopic properties of these

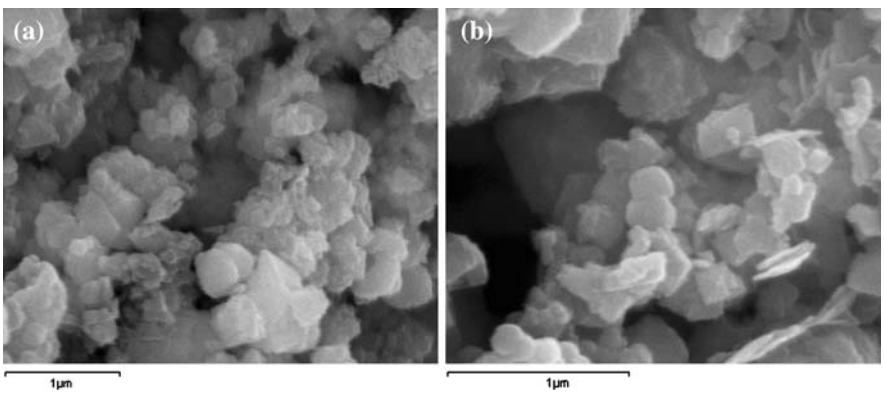

Fig. 2 Scanning electron micrographs taken from the surface of the catalytic precursors: (**a**) 4NiO–MgO, (**b**) 4NiO–MgOr

Table 2 Characterization of the catalysts

Catalysts	Crystalline phases (XRD)	Metallic areas (m^2/g)
Ni	Ni	1.7
NiMgO	Ni, MgO	0.9
4NiMgO	Ni, MgO	0.6
NiMgOr	Ni, $Mg(OH)_2$	0.4
4NiMgOr	Ni, $Mg(OH)_2$	0.2
NiMgOa	Ni, MgO	0.9
4NiMgOa	Ni, MgO	1.2

basic compounds [16, 17]. This involves, indirectly, a sintering of the metallic particles. For the samples with MgOr, their lower metallic area could be explained by a higher agglomeration due to the additional water formed by dehydroxylation of the surface hydroxyl groups. For the catalyst NiMgO, lower agglomeration and, consequently, higher metallic area can be expected, due to the more efficient water removing in this system, which presents lower reducibility (Table 1).

3.2 Basicity Study of the Catalytic Precursors and Catalysts by CO_2-TPD

In order to characterize the basic properties of the catalytic precursors and catalysts, the strength distribution of their basic sites were determined by TPD-MS of preadsorbed carbon dioxide.

Figure 3 shows the CO_2-TPD profiles of commercial MgO, sample NiO and the catalytic precursors 4NiOMgO and NiOMgO. The TPD profile of commercial MgO mainly shows two intense desorption peaks at 280 and at 600 °C whereas the TPD profile of the NiO sample shows only one desorption peak around 420 °C. For the 4NiO-MgO and NiOMgO precursors, obtained by physical mixing of the NiO sample and commercial MgO in the appropriate amounts, we can observe two desorption peaks with different intensity and position respect to the peaks of the TPDs of commercial MgO and sample NiO. This could be explained taking into account the NiO/MgO ratio of the catalytic precursors and the existence of some interaction between NiO and MgO.

Figure 4 shows the CO_2-TPD profiles of rehydrated MgO (MgOr), the catalytic precursors NiOMgOr and 4NiOMgOr, and also of the NiO sample for comparison. The TPD profile of sample MgOr shows four desorption peaks: a medium-intense peak around 300 °C, which is a shoulder of the highest-intense peak appeared at 390 °C, a very low intense peak at 440 °C, and a peak with medium intensity at 600 °C. The catalytic precursors 4NiOMgOr and NiOMgOr show some changes in the position and intensity of the desorption peaks respect to the MgOr and NiO TPDs. Again, the different NiO/MgOr ratio and the presence of some NiO/$Mg(OH)_2$ interaction could explain these results.

Figure 5a shows the CO_2-TPD profile of catalyst NiMgO. The peaks in this thermogram have been assigned by comparison with the thermogram of commercial MgO (Fig. 3) and the thermogram obtained for the Ni sample without MgO (Fig. 5b). In the TPD profile of the NiMgO catalyst, we can mainly see two desorption peaks: one with low intensity at 330 °C, which can be assigned by intensity and position to metallic nickel (see Fig. 5b), and a peak with medium intensity at 600 °C which can be related to the stronger basic sites of magnesia (see Fig. 3). When it is compared with the CO_2-TPD profile of MgO, we observe that the intense peak at 280 °C, corresponding to the weakest basic sites of commercial magnesia, now does not appear. This fact, together with the presence of the desorption peak characteristic of metallic nickel let us to think that the metallic nickel particles formed by the NiO reduction should cover the weakest basic sites of MgO in catalyst NiMgO, explaining the disappearance of this peak. These results suggest the existence of some interaction between the nickel and the weakest basic sites of

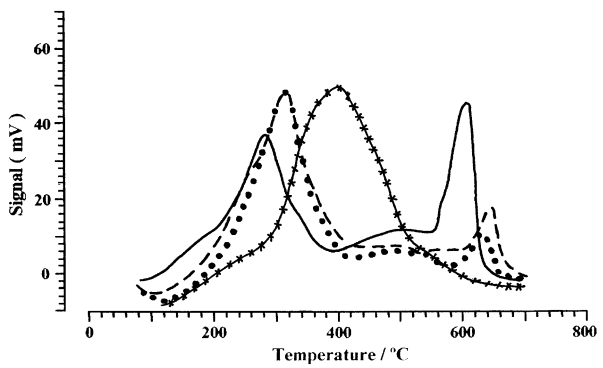

Fig. 3 CO_2-TPDs of the samples: MgO (—), NiO (××××), 4NiOMgO (●●●●) and NiOMgO (- - - -)

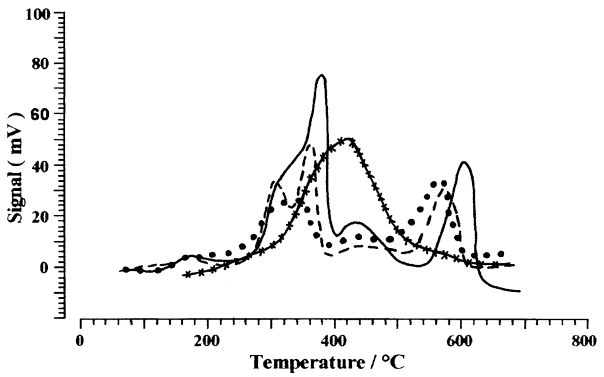

Fig. 4 CO_2-TPDs of the samples: MgOr (—), NiO (××××), 4NiOMgOr (●●●●) and NiOMgOr (- - - -)

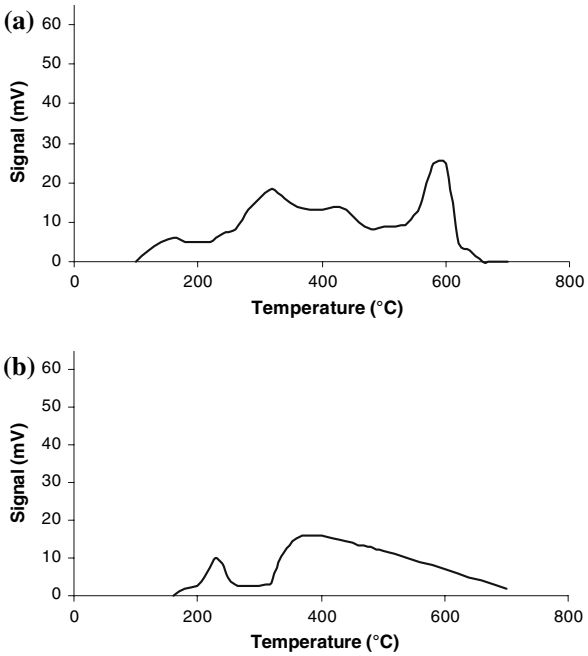

Fig. 5 CO_2-TPDs of the catalysts (**a**) NiMgO and (**b**) Ni

magnesia. As other authors have reported, CO_2 interacts with nickel being this interaction weaker when the nickel sites increase their electronic density in the presence of other oxide species [18]. This could explain the shift of the CO_2 desorption peak assigned to Ni sites at lower temperatures in the TPD of NiMgO (330 °C) respect to the same peak observed in the TPD of the Ni sample (370 °C). Lastly, the peak desorbed at 600 °C (Fig. 5a) has similar intensity and similar desorption temperature to that of commercial magnesia (Fig. 3) taking into account the different MgO amount present in the two samples. This means that Ni particles do not interact practically with the stronger basic sites of magnesia.

Figure 6 shows the CO_2-TPD profile of catalyst NiMgOr. For the catalysts with rehydrated magnesia, the CO_2-TPD profiles are very similar to that of the rehydrated magnesia (Fig. 4). However, a new peak appears around 340 °C (between the peaks at 300 and 390 °C observed in the TPD profile of sample MgOr) that could be related to nickel sites interacting with basic sites or to basic sites of $Mg(OH)_2$ which are covering some nickel particles. Both situations involve a certain interaction between the Ni and the brucite particles.

Lastly, the CO_2-TPD profile of NiMgOa catalyst presents three desorption peaks at 280, 370, and 620 °C (Fig. 7). The peaks that desorbs around 280 and 600 °C are proportional in intensity (taking into account the magnesia amount) to those of commercial magnesia (Fig. 3) whereas the peak around 370 °C can be associated to metallic nickel (Fig. 5b), as commented above. Consequently, the interaction Ni–MgO practically does not exist. All these results will be correlated later with the catalytic activity data.

3.3 Catalytic Activity

Figure 8 shows the catalytic activity for all catalysts in the hydrogenation of styrene oxide. Catalysts with commercial MgO present the best conversion and the best selectivity to 2-phenylethanol values arriving to 100% for the catalyst with more magnesia content, NiMgO. These values are higher than those obtained for the rest of catalysts. By using NiMgOr and 4NiMgOr catalysts, much lower conversion and lower selectivity to 2-phenylethanol values (Fig. 8) at expenses of higher amounts of condensation products were observed. Finally, catalysts NiMgOa and 4NiMgOa (with very low nickel–magnesia interaction and higher metallic area values) show low conversion and very low or null selectivity to 2-phenylethanol (Fig. 8).

The metallic area of the catalysts cannot explain these catalytic results, since the highest metallic area (1.2 m^2/g) corresponds to the catalyst 4NiMgOa, which gives to low conversion and very low selectivity to 2-phenylethanol. Interestingly, these catalytic behaviours could be related to the different CO_2-TPD profiles observed for these catalysts. Thus, the catalyst with higher MgO content (NiMgO), whose CO_2-TPD showed metallic nickel partially covering

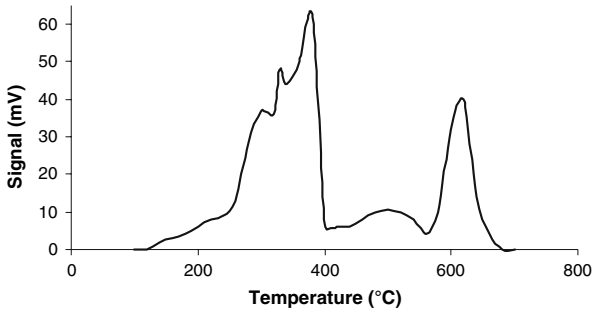

Fig. 6 CO_2-TPD of the catalyst NiMgOr

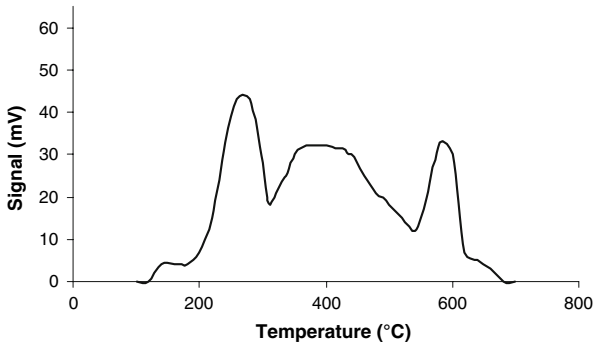

Fig. 7 CO_2-TPD of the catalyst NiMgOa

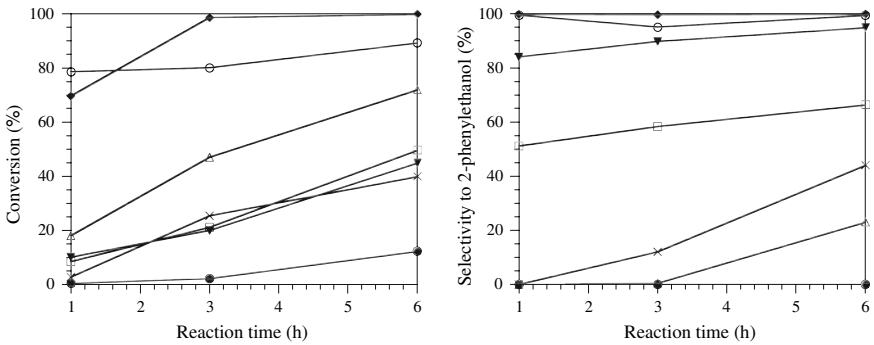

Fig. 8 Catalytic activity of the catalysts for the hydrogenation of styrene oxide. Symbols: NiMgO (♦), 4NiMgO (◯), NiMgOr (×), 4NiMgOr (□), NiMgOa (●), 4NiMgOa (Δ), and Ni (▼)

the weakest basic sites of magnesia (Fig. 5a) is more active and more selective to 2-phenylethanol than the rest of catalysts. On the other hand, the CO_2-TPDs of catalysts NiMgOr and NiMgOa showed an important amount of available basic sites that favour the formation of higher amounts of condensation products, which are responsible for the catalyst deactivation [13]. In these Ni–MgOr and Ni–MgOa systems the interaction between metallic and basic particles are very low or null. Therefore, we can conclude that the metallic nickel under the influence of the weakest basic sites of commercial magnesia should be related to the selective formation of 2-phenylethanol. This minimizes the formation of other reaction products, such as ethylbenzene or condensation products, which were not detected for these catalysts.

The catalytic lifetime of the best catalyst (NiMgO) was also tested (Fig. 9). After reusing the catalyst once, the same conversion and selectivity values were obtained. When the catalyst is used again we observe a slight conversion decrease from 100 to 83%, whereas the selectivity to 2-phenylethanol remains around 95%. These values are maintained after reusing the catalyst three more times. These slight variations could be explained by the formation of small amounts of condensation products, which block some metallic sites. Therefore, there is a clear influence of basicity in the catalytic behaviour of these Ni–MgO systems.

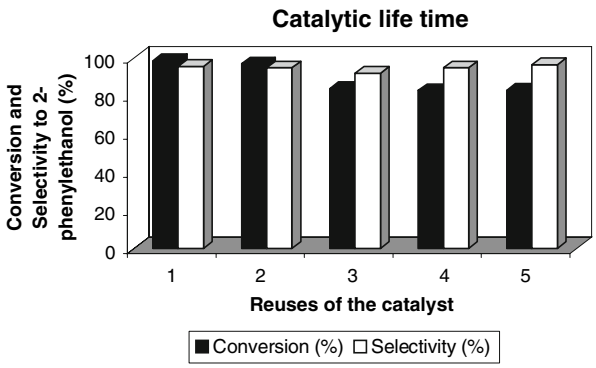

Fig. 9 Catalytic lifetime of the catalyst NiMgO

4 Conclusions

The basic sites available in the prepared catalysts determine the distribution of the reaction products for the hydrogenation of styrene oxide. The catalysts prepared by mixing commercial magnesia with the NiO sample and later reduction give to the higher conversion and higher selectivity to 2-phenylethanol values. The CO_2-TPD profile of the best catalyst, NiMgO, (100% conversion and 100% selectivity to 2-phenylethanol) showed the disappearance of the peak corresponding to the weaker basic sites of commercial magnesia. This means that the metallic nickel, obtained after reduction, cover these basic sites and, therefore, there is some influence between the nickel particles and the basic sites, which become less available. The existence of a certain interaction between the nickel and the weakest basic sites of magnesia in these Ni–MgO catalysts favour the quickly formation of 2-phenylethanol, and consequently, minimizes other side reactions like the formation of condensation products. The catalyst prepared with the highest amount of commercial magnesia (NiMgO) maintains high conversion and selectivity to 2-phenylethanol values after reusing several times.

On the other hand, the CO_2-TPD profiles obtained for catalysts NiMgOr and NiMgOa showed that they have higher amounts of basic sites available. This can explain the higher amounts of condensation products, detected for catalysts NiMgOr, 4NiMgOr, NiMgOa and 4NiMgOa, which are responsible for their lower activity.

Acknowledgments The authors are grateful for the financial support of the "Ministerio de Ciencia y Tecnología" and FEDER funds (REN2002-04464-C02-02).

References

1. Mookherjee BD, Wilson RA (1994) Kirk-Othmer encyclopedia of chemical technology, 4th edn., vol. 17. John Wiley & Sons, New York
2. Ernst T (1982) Theimer in fragrance chemistry. Academic Press, New York
3. Chaudari RV, Telkar MM, Rode CV (2000) US Patent 6,166,269

4. Bauer K, Garbe D, Surburg H (1990) Common fragrance and flavour materials. New York
5. Olah GA, Prakash Reddy V, Surya Prakash GK (1994) Kirk-Othmer encyclopedia of chemical technology, 4th edn., vol. 11. John Wiley & Sons, New York
6. Wood TF, Clifton NJ (1950) US Patent 2,524,096
7. Hopff H, Kuhn H, Hoffmann U, Hamburg B (1958) US Patent 2,822,403
8. Mitsui S, Imaizumi S, Hisashige M, Sugi Y (1973) Tetrahedron Lett 29:4093
9. Yadav VG, Chandalia SB (1998) Org Process Res Dev 2:294
10. Kochkar H, Clacens JM, Figueras F (2002) Catal Lett 78:91
11. Rathouský J, Zukal A, Stárek J (1993) Appl Catal A Gen 94:167
12. Schaper H, Berg-Slot JJ, Stork WHJ (1989) Appl Catal A Gen 54:79
13. Bergada O, Salagre P, Cesteros Y, Medina F, Sueiras JE (2004) Appl Catal A Gen 272:125
14. Thomasson P, Tyagi OS, Knözinger H (1999) Appl Catal A Gen 181:181
15. Hattori H (2004) J Jpn Petrol Inst 47:67
16. Serra M, Salagre P, Cesteros Y, Medina F, Sueiras JE (2000) Solid State Ionics 134:229
17. Schaper H, Berg-Slot JJ, Stork VHJ (1989) Appl Catal 54:79
18. Xiancai L, Min W, Zhihua L, Fei H (2005) Appl Catal A Gen 290:81